

See discussions, stats, and author profiles for this publication at: <https://www.researchgate.net/publication/230857493>

# Theoretical Investigation on the Steric Interaction in Colloidal Deposition

ARTICLE in LANGMUIR · SEPTEMBER 2012

Impact Factor: 4.46 · DOI: 10.1021/la302201g · Source: PubMed

---

CITATIONS

6

---

READS

52

## 2 AUTHORS:



[Shihong Lin](#)

Vanderbilt University

29 PUBLICATIONS 524 CITATIONS

SEE PROFILE



[Mark Wiesner](#)

Duke University

265 PUBLICATIONS 10,828 CITATIONS

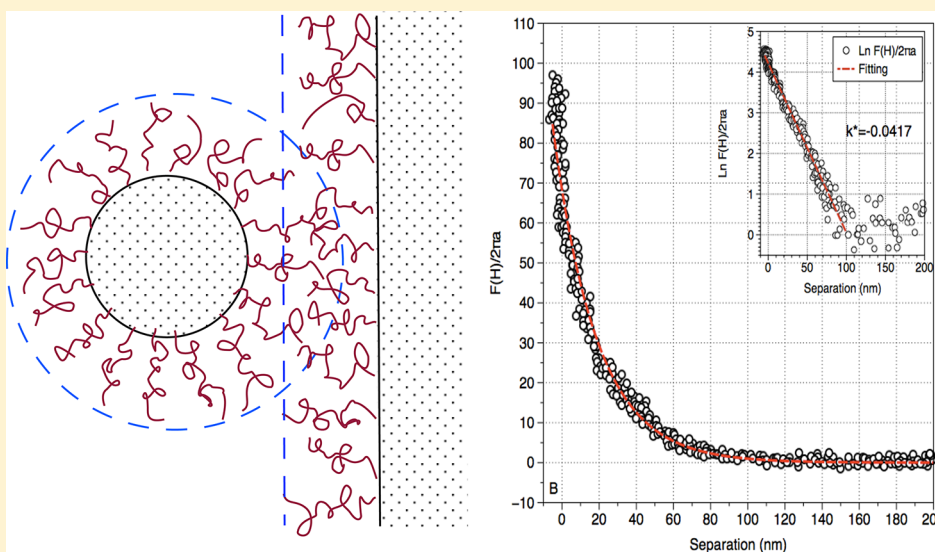
SEE PROFILE

# Theoretical Investigation on the Steric Interaction in Colloidal Deposition

Shihong Lin and Mark R. Wiesner\*

Department of Civil and Environmental Engineering, and Center for the Environmental Implications of NanoTechnology (CEINT), Duke University, PO Box 90287, Durham, North Carolina 27708, United States

**S** Supporting Information



**ABSTRACT:** A theoretical investigation was conducted upon the steric interaction between a spherical particle and a flat plate. The effects of curvature on both the segment density distribution of polymer and on the steric interaction energy between a particle and a plate were examined. It was found that the conventional approach using Derjaguin approximation may overestimate the interaction energy, especially for very small particles. Based on the results obtained from applying the Flory–Krigbaum theory with the accurate geometry change during the interaction, simple approximate expressions of exponential form were proposed for both the osmotic (mixing) and elastic contributions to the steric interaction energy for a sphere–plate interaction. The proposed model was validated against a set of experimental results from a reported study employing atomic force microscopy. Also investigated was the steric interaction between a spherical particle coated with polymer and an uncoated flat surface. It was found that the steric interaction energy from the osmotic contribution is significantly higher than that from the elastic contribution and that steric interaction is considerably weaker when the polymer exists on only one of the interacting surfaces.

## INTRODUCTION

The steric interaction is of critical importance in controlling the stability of colloidal particles. With both osmotic and elastic contributions, steric interaction is found to be very robust in stabilizing particles against aggregation and deposition.<sup>1,2</sup> Its robustness is not only reflected in its strength as compared to that of the electrical double layer (EDL) interaction but also in its relative insensitivity to the variation of solution chemistry: neither ionic strength, which affects double layer screening, nor changes in the surface potential can significantly affect the efficacy of steric stabilization, so long as these changes do not considerably impact the goodness of the solvent for the coating polymer.<sup>1,2</sup> For this reason, steric stabilization is widely employed in the synthesis or preparation of colloidal particle

suspensions.<sup>3–6</sup> The steric interaction between adsorbed natural organic matter (NOMs) has also been found to play an important role in enhancing the stability and mobility of colloidal particles in aqueous environment.<sup>7–12</sup> Interaction between a colloidal particle and a much larger macroscopic environmental surface can be described as an interaction between a sphere and a plate.<sup>13,14</sup> Therefore, a quantitative description of the steric interaction of a sphere–plate system, which allows improved understanding of the particle–surface interaction, is important in assessing the stability and transport

**Received:** May 30, 2012

**Revised:** September 12, 2012

**Published:** September 15, 2012

of colloidal particles. It is thus the purpose of this paper to propose expressions that describe the steric interaction in colloidal particle deposition, and to discuss the effect of large curvature of a nanoparticle on its steric interaction in such a context. The early theoretical studies on steric interaction between adsorbed polymer layers were conducted for interaction between two flat plates, which yield interaction energy per area of flat plates.<sup>3,15–19</sup> The results of these studies are commonly scaled to a sphere–sphere interaction via Derjaguin approximation (DA) which is also widely employed to scale EDL and van der Waals (vdW) interactions from a plate–plate geometry to systems of other geometries.<sup>20</sup> For an interaction between two spherical particles of different sizes, the DA is given as

$$\Delta G_{\text{SS,DA}}(H) = 2\pi \left( \frac{a_1 a_2}{a_1 + a_2} \right) \int_h^\infty \Delta G_{\text{PP}}(H) dH \quad (1)$$

where  $\Delta G_{\text{SS,DA}}(H)$  is the Gibbs free energy of interaction (or shortly, interaction energy) calculated with the DA for two particles of radii  $a_1$  and  $a_2$  separated by a distance  $h$ , and  $\Delta G_{\text{PP}}(H)$  is the interaction energy per area between two parallel plates separated by a distance  $h$ . For interactions between a particle and a plate, one of the radii becomes infinity, in which case the following expression is obtained:<sup>21</sup>

$$\Delta G_{\text{SP,DA}}(H) = 2\pi a \int_h^\infty \Delta G_{\text{PP}}(H) dH \quad (2)$$

where  $\Delta G_{\text{SP,DA}}(H)$  is the interaction energy between a particle of radius  $a$  and a plate based on the DA. It is well-known that the geometric simplification employed renders the DA applicable only when the interaction range is small compared to the size of the particle. For example, for the EDL interaction, the proper application of DA requires that the double layer thickness or the Debye length ( $1/\kappa$ ) is very thin compared to the size of the particle<sup>22–24</sup> (i.e.,  $\kappa a \gg 1$ ).

There is no exception for steric interaction: the expressions based on DA (eqs 1 and 2) are only applicable to relatively large particles (small curvature) with a relatively thin coating layer, because of the geometric simplification involved in deriving these equations. This problem is aggravated by the fact that, with a particle of large curvature, the segment density distribution of polymer varies significantly in the radial direction. The segment density should be much lower at the periphery of the coating shell than at the vicinity of the core particle or the flat surface. The accurate description of a polymer layer tethered to a highly curved surface may be described by the self-consistent field analysis.<sup>25,26</sup> As physical overlapping (interpenetration) is mathematically represented by the correlation of segment density distribution functions, the scaling of the plate–plate interaction energy to a sphere–plate system may be problematic because their profiles of segment density distribution might be very different. Finally, in the scenarios where it may be appropriate to apply DA to evaluate  $\Delta G_{\text{SS,DA}}(H)$  and  $\Delta G_{\text{SP,DA}}(H)$ , it has to be noted that, unlike EDL or vdW interactions,  $\Delta G_{\text{PP}}(H)$  is zero when  $H > 2\delta$  for steric interaction. Therefore, although the upper limit of integration can be theoretically set to infinity, the actual integration is only physically meaningful to a separation  $H$  corresponding to a ring where the overlapping vanishes.

For a sphere–sphere interaction, which is of strong relevance in colloidal stability, improved theories that avoid the application of the DA have been proposed to obtain better

evaluation of the energy of steric interaction. These theories include, but are not limited to, the strong-stretching theory (SST)<sup>27,28</sup> and the self-consistent field theory (SCFT)<sup>29,30</sup> that consider the details of segment density distribution and of polymer deformation during interaction. With these sophisticated theories, the effect of chain tilting during the interaction can also be taken into account.<sup>25</sup> Although these models provide useful insights into the phenomenon of steric interaction, the application of these models is limited by the fact that only numerical solutions of these models are available. Lozsan et al. found that a model based on the Flory–Krigbaum theory assuming uniform segment density distribution (it was called extended Vincent (EV) model by the authors) could quantitatively describe the steric interaction between two spherical particles with satisfactory accuracy,<sup>31</sup> which indicates that simple mathematical descriptions are available to yield sufficient approximation for estimating the steric interaction energy.

In this work, an approach similar to that employed by Lozsan<sup>31</sup> is used to model the steric interaction between a sphere and a flat plate using the Flory–Krigbaum theory with a uniform segment density assumption. Two different regimes of the interaction—the interpenetration (only) regime and the interpenetration plus compression regime—were modeled separately but the transition was mathematically continuous. Even though the application of the Flory–Krigbaum theory is mathematically straightforward, the resulting equations for interaction energy were still cumbersome due to the complicated expressions needed to describe the geometry change during the interaction, especially with the compression domain. For practical purpose, simple approximate expressions were proposed that based on the results of the full expressions.

## ■ SEGMENT DENSITY DISTRIBUTION AROUND A SPHERICAL PARTICLE

One of the widely employed theories in describing the steric interaction between polymer layers is the Flory–Krigbaum theory,<sup>15,31</sup> which needs no detailed repetition here. The segment density distribution is required in order to apply the Flory–Krigbaum theory to obtain the interaction energy due to polymer mixing (or interpenetration). For a polymer-coating layer on a flat plate, Vincent et al. proposed several possible models to describe the segment density distribution.<sup>16</sup> Among all of these models, the uniform distribution is the simplest and possibly the only model that allows for a simple analytical expression for steric interaction, whereas the pseudotails model may more appropriately describe the realistic segment density distribution. The expressions for these two models are given as eqs 3 and 4

$$\text{uniform } \phi_{\text{FP}}(z) = \bar{\phi} \quad (3)$$

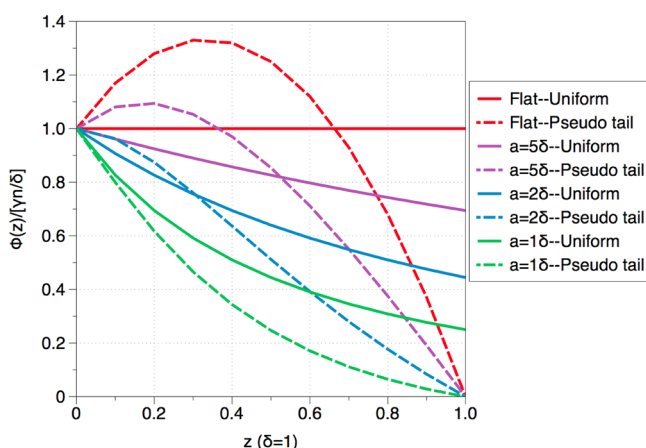
$$\text{pseudotail } \phi_{\text{FP}}(z) = \bar{\phi} \left( 1 + \frac{2z}{\delta} - \frac{3z^2}{\delta^2} \right) \quad (4)$$

where  $a$  is the particle radius,  $z$  is the radial position starting from the particle surface,  $\delta$  is the coating thickness, and  $\bar{\phi}_p$  is the average segment density of the coating layer. The curvature of a spherical particle will drastically change the segment density distribution profile, especially when the particle is small. Assuming the radial segment density distribution of a single polymer chain on a spherical particle remains the same as that

on a plate, the segment density distribution of the spherical polymer shell is then given as

$$\phi_s(z) = \phi_{FP}(z) \frac{a^2}{(a+z)^2} \quad (5)$$

According to this model, when the core particle size  $a$  is small, the effect of curvature as described by the term  $a^2/[(a+z)^2]$  will dominate the original flat-plate-based distribution  $\rho_{FP}(z)$  on the dependence on  $z$ . Specifically, with the pseudotail model, when the radius of the core particle  $a$  is less than  $5\delta$ , the segment density maximum at an intermediate distance away from the surface, which is characteristic of a pseudotail model on a flat plate, disappears due to the curvature effect (Figure 1).



**Figure 1.** Effect of relative curvature ( $a/\delta$ ) on segment density distribution. Solid curves represent uniform distribution along radial direction. Dashed curves represent pseudo tail distribution along radial direction.

Regardless of the initial segment density distribution on the flat plate, the effect of curvature invariably lowers the segment density, more significantly the further away from the spherical surface.

## ■ INTERPENETRATION DOMAIN

As long as the coating layer starts to interpenetrate ( $z \leq 2\delta$ ), osmotic repulsion results from reduced configuration entropy of the overlapping layers. Based on the Flory–Krigbaum theory,<sup>3,15,31</sup> the Gibbs free energy associated with interpenetration (or mixing) of two polymer layers is given by

$$\Delta G_{\text{mix}}(H) = 2k_B T \left( \frac{V_p^2}{v_s} \right) \left( \frac{1}{2} - \chi \right) \times \left( \int \phi_1 \phi_2 dV \right) \delta < H \leq 2\delta \quad (6)$$

where  $V_p$  is the volume of the polymer,  $v_s$  is the volume of a solvent molecule,  $\chi$  is the Flory–Huggins solvency parameter, and  $\phi_1$  and  $\phi_2$  are the segment density distribution functions of the two interacting polymer layers, respectively. The integral  $\int \phi_1 \phi_2 dV$  is evaluated over the interpenetration zone. To derive an analytical expression using eq 6, a simple segment density distribution, such as a uniform distribution, has to be assumed.<sup>31</sup> While it is understood that in reality a uniform distribution is unlikely for coatings on a spherical particle or a flat plate,<sup>32</sup> this highly simplified case is sufficient to illustrate the effect of curvature and the DA on the interaction energies

and to yield reasonably accurate expressions for calculating interaction energy

Assuming that the number of adsorbed or anchored polymer chains per area is  $\gamma$ , the number of monomers per polymer chain (polymerization degree) is  $n$ , and the coating thickness is  $\delta$ , then the segment density of a uniformly distributed polymer layer on a flat surface is simply

$$\phi_{FP}(z) = \bar{\phi} = \frac{\gamma n}{\delta} \quad (7)$$

Note that, although such a definition of segment density is straightforward for a polymer brush with  $\gamma$  being the area density of anchoring sites, it is universally applicable to describe polymer layers of other configuration as long as  $\gamma$  is defined as the number of polymer chains (not necessarily anchoring or adsorption sites, as a polymer chain may have multiple fixation sites) per surface area.

With the curvature effect, the segment density distribution of a polymer layer on a spherical particle of radius  $a$  is then given by

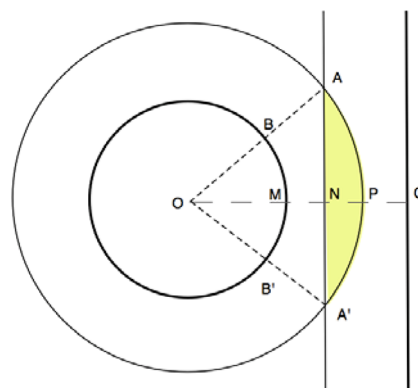
$$\phi_s(z) = \bar{\phi} \frac{a^2}{(a+z)^2} = \frac{\gamma n}{\delta} \frac{a^2}{(a+z)^2} \quad 0 < z \leq \delta \quad (8)$$

which can be written more conveniently as a function of radius  $r = a + z$

$$\phi_s(z) = \frac{\gamma n a^2}{\delta} \frac{1}{r^2} \quad a < r \leq \delta + a \quad (9)$$

Based on eqs 1, 5, and 7, the Gibbs free energy associated with interpenetration between a spherical and a flat polymer layer can be written as

$$\Delta G_{\text{mix}}(H) = 2k_B T \left( \frac{V_p^2}{v_s} \right) \left( \frac{1}{2} - \chi \right) \frac{\gamma n a^2}{\delta} \int \frac{1}{r^2} dV \quad (10)$$



**Figure 2.** Interpenetration zone (yellow region). It is assumed that the thicknesses of the coating layer for the plate (NQ) and for the sphere (BA) are both  $\delta$ . The radius of the particle is  $a$  (OB). The separation distance is  $H$  (MQ).

For the geometry of the interpenetration zone, it is more convenient to evaluate the integral in eq 10 using a cylindrical coordinate system  $(p, q, \theta)$  in which the coordinate of a point in the coating layer corresponding to radius  $r$  will become  $(p, q)$ , with  $p$  being the radius and  $q$  being the height and all angular parameters are ignored due to geometric symmetry. In such a coordinate  $r$  would become

$$r^2 = p^2 + q^2 \quad (11)$$

The analytical solution to the integral in eq 10 over a spherical cap of height  $h$  (the interpenetration zone) is

$$\begin{aligned} \int \frac{1}{r^2} dV \Big|_{\text{mix}} &= \int_0^{2\pi} d\theta \int_{R-h}^R \left( \int_0^{\sqrt{R^2-q^2}} \frac{1}{p^2+q^2} p dp \right) dq \\ &= 2\pi \left[ h - (R-h) \ln \left( \frac{R}{R-h} \right) \right] \end{aligned} \quad (12)$$

where  $R = a + \delta$  is the overall radius of the coated particle and  $h$  is the height of the overlapping region ( $h = 2\delta - H$ ). Consequentially, the analytical expression for the steric interaction between a particle of radius  $a$  coated with a polymer layer of thickness  $\delta$  and a flat surface coated with the same coating layer, within the interpenetration zone ( $\delta \leq H < 2\delta$ ), is given as

$$\begin{aligned} \Delta G_{\text{mix,SP}} &= 4\pi k_B T \left( \frac{V_P^2}{v_S} \right) \left( \frac{1}{2} - \chi \right) \left( \frac{\gamma n a}{\delta} \right)^2 [(2\delta - H) \\ &\quad - (a + H - \delta) \ln \left( \frac{a + \delta}{a + H - \delta} \right)] \end{aligned} \quad (13)$$

It is instructive to compare eq 13 to that obtained using DA. To do that, the per-area plate–plate interaction energy between two uniformly distributed polymer layers on two flat surfaces is first evaluated based on eq 1

$$\Delta G_{\text{mix,PP}} = 2\pi k_B T \left( \frac{V_P^2}{v_S} \right) \left( \frac{1}{2} - \chi \right) \left( \frac{\gamma n}{\delta} \right)^2 (2\delta - H) \quad (14)$$

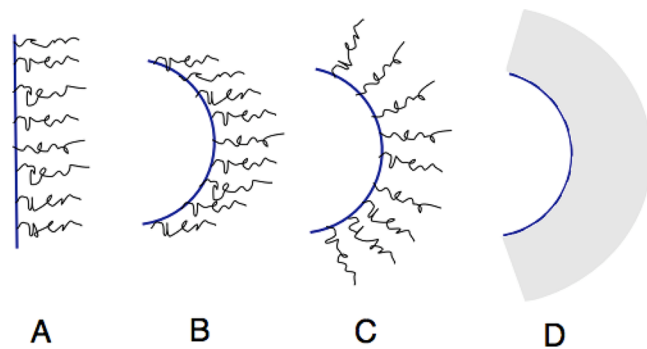
By applying the DA while keeping in mind that the scaling can only be conducted to the fringe of interpenetration zone, the following expression for the energy of a sphere–plate steric interaction is obtained:

$$\begin{aligned} \Delta G_{\text{mix,SP}}^{\text{DA}} &= \frac{2}{3} \pi k_B T \left( \frac{V_P^2}{v_S} \right) \left( \frac{1}{2} - \chi \right) \left( \frac{\gamma n a}{\delta} \right)^2 (2\delta - H)^2 \\ &\quad (H + 3a + \delta) \end{aligned} \quad (15)$$

The differences between eqs 13 and 15 are simply due to the effect of curvature on segment density distribution. To quantify such an effect, we define a parameter  $\beta_{\text{DA}}$  (Figure 3, panel C vs B) as

$$\begin{aligned} \beta_{\text{DA}}(a, \delta, H) &= \frac{\Delta G_{\text{mix,SP}}}{\Delta G_{\text{mix,SP}}^{\text{DA}}} \\ &= \frac{6a^2 \left[ (2\delta - H) - (a + H - \delta) \ln \left( \frac{a + \delta}{a + H - \delta} \right) \right]}{(2\delta - H)^2 (H + 3a + \delta)} \end{aligned} \quad (16)$$

The expression based on DA inevitably overestimates the interaction as it assumes the same segment density at the periphery of the coating shell as that on the core surface. One simple way to improve the constant-segment-density approximation implicit in employing DA, is to use a segment density averaged over the coating shell ( $\rho_{\text{S,avg}}$ ) based on the distribution given by eq 9:



**Figure 3.** Graphical illustration of the segment density distributions based on different models. (A) Uniform distribution on a flat plate. (B) Uniform distribution in a spherical shell with the same segment density as that on a flat plate. This is the segment density distribution for a sphere if Derjaguin approximation is applied. (C) Uniform distribution only along the radial direction, as described by eq 9. (D) Uniform distribution in a spherical shell with the mean segment density of panel C over the volume of the spherical shell.

$$\phi_{\text{S,avg}} = \frac{3\gamma n a^2}{(a + \delta)^3 - a^3} = \frac{3a^2\delta}{(a + \delta)^3 - a^3} \frac{\gamma n}{\delta} = \eta \frac{\gamma n}{\delta} \quad (17)$$

where  $\eta$  is a curvature correcting factor defined as

$$\eta = \frac{3a^2\delta}{(a + \delta)^3 - a^3} \quad (18)$$

With  $\phi_{\text{S,avg}}$  replacing  $\phi_{\text{FP}}$ , the interaction energy due to interpenetration is given by

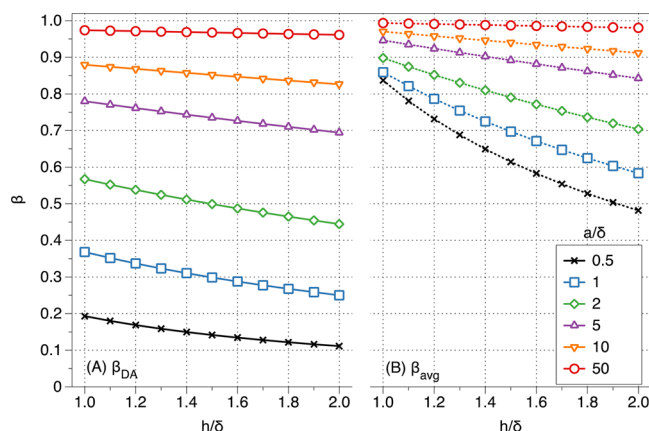
$$\begin{aligned} \Delta G_{\text{mix,SP}}^{\text{avg}} &= 2\pi k_B T \left( \frac{V_P^2}{v_S} \right) \left( \frac{1}{2} - \chi \right) \left( \frac{\gamma n}{\delta} \right)^2 (2\delta - H)^2 \\ &\quad (H + 3a + \delta) \frac{a^2\delta}{(a + \delta)^3 - a^3} \end{aligned} \quad (19)$$

which is different from eq 15 simply by a factor of  $\eta$ . Similarly, it is possible to quantify the goodness of such an approximation using a comparison parameter  $\beta_{\text{avg}}$  (Figure 3, panel D vs B) as defined as

$$\begin{aligned} \beta_{\text{avg}}(a, \delta, H) &= \frac{\Delta G_{\text{mix,SP}}}{\Delta G_{\text{mix,SP}}^{\text{avg}}} \\ &= \{6(3a^2 + 3a\delta + \delta^2) \left[ (2\delta - H) \right. \\ &\quad \left. - (a + H - \delta) \ln \left( \frac{a + \delta}{a + H - \delta} \right) \right] \} \\ &\quad / \{ (2\delta - H)^2 (H + 3a + \delta) \} \end{aligned} \quad (20)$$

Note that  $\Delta G_{\text{mix,SP}}$ ,  $\Delta G_{\text{mix,SP}}^{\text{DA}}$ , and  $\Delta G_{\text{mix,SP}}^{\text{avg}}$  given above are all only valid for  $\delta \leq H < 2\delta$  as they are developed for the interpenetration domain. Arbitrarily setting  $\delta$  as 1 and describe  $a$  in the unit of  $\delta$ , we show the effect of curvature on  $\beta_{\text{DA}}$  and  $\beta_{\text{avg}}$  in Figure 4: using  $\phi_{\text{S,avg}}$  instead of  $\phi_{\text{FP}}$  significantly improves the approximation by better incorporating the effect of curvature, although for small particles with thick coating layer the deviations are still large, only when  $a > 10\delta$  can the deviation be kept within 10% throughout the interaction.





**Figure 4.**  $\beta$  at different particle sizes for models using two different uniform segment densities ( $\phi_{FP}$  and  $\phi_{S,avg}$ ). A lower value means more severe overestimation by the uniform segment density model ( $\Delta G_{mix,SP}^{DA}$  and  $\Delta G_{mix,SP}^{avg}$ ) as compared to the reference model  $\Delta G_{mix,SP}$ .

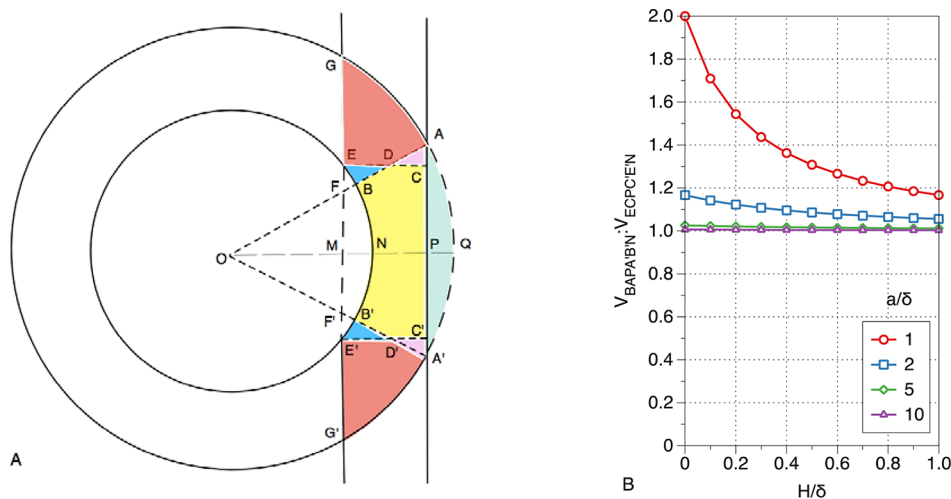
## ■ INTERPENETRATION PLUS COMPRESSION DOMAIN

It was assumed that the polymer coatings do not deform in the interpenetration domain (thus the segment density distribution contributed from each layer remains unchanged) and that the repulsive energy stems only from the osmotic pressure due to mixing of polymers in a good solvent.<sup>33</sup> When the separation is smaller than the coating thickness ( $H < \delta$ ), the interacting coating-polymers have to deform due to geometric constraints. Both interpenetration and intrapenetration (self-penetration) must be considered, in which case the full expression for the Flory–Krigbaum theory has to be used:<sup>15,31</sup>

$$\Delta G_{mix}(H) = k_B T \left( \frac{V_p^2}{v_s} \right) \left( \frac{1}{2} - \chi \right) \left( \int (\phi_1^2 + 2\phi_1\phi_2 + \phi_2^2)_H dV - \int \phi_{1,\infty}^2 dV - \int \phi_{2,\infty}^2 dV \right) \quad (21)$$

where  $\phi_1$  and  $\phi_2$  are the segment density of the two interacting polymer layers at a given point when the separation is  $H$  and  $\phi_{1,\infty}$  and  $\phi_{2,\infty}$  are the same parameters when the polymer layers are not interacting. The integrals are technically evaluated throughout the whole space. However, since the segment density of the noninteracting portions remains unchanged, for convenience the integrals can be evaluated only for the overlapping and compressed regions.

The deformation of polymer layers in the compression domain is complicated. In order to obtain a practically simple analytical expression, uniform segment density distributions again are assumed for both the flat and spherical layers of the polymer. Figure 5 gives a simplified view of different domains of overlapping when  $H < \delta$ . If we assume that the polymer chains can only retract in the direction normal to the surface (either particle or plate), i.e., if we ignore the effect of tilting, then with compression the geometric change in the spherical coating is from BAQA'B'N (green + yellow + pink) to BAPA'B'N (yellow + pink) and the geometric change in the flat coating layer is from EME'CP'C (yellow + blue + white) to ECC'E'N (yellow + blue). Denoting the unperturbed segment density of the spherical coating and the flat coating as  $\phi_{S,avg,\infty}$  and  $\phi_{FP,\infty}$ , respectively, and the segment density of the spherical coating and the flat coating in the compressed region as  $\phi_{S,avg,H}$  and  $\phi_{FP,H}$ , then we will have  $\phi_1\phi_2 = \phi_{S,avg,\infty}\phi_{FP,\infty}$  in the red region,  $\phi_1\phi_2 = \phi_{S,avg,\infty}\phi_{FP,H}$  in the blue region,  $\phi_1\phi_2 = \phi_{S,avg,H}\phi_{FP,\infty}$  in the pink region, and  $\phi_1\phi_2 = \phi_{S,avg,H}\phi_{FP,H}$  in the yellow region. However, such a detailed classification of interaction domains inevitably yields significant, yet unnecessary, complexity to solving the integral defined in eq 21, especially considering the fact the even by solving the integral this way the solution would not be exact because of two aforementioned simplifying assumptions: (1) uniform segment density distribution and (2) only retraction normal to the surface is allowed. A simplified domain classification is thus preferred for obtaining a practical analytical expression. Therefore we classify the interacting region into two domains: (1) the interpenetration domain, which involves no compressed polymer, is given by region GACDE and G'A'C'D'E' (red + pink, they are the same connecting region) in Figure 5A and (2) the compression domain, the segment density of which increases with decreasing  $H$ , is given by ECPC'E'N (yellow +



**Figure 5.** (A) Volume ratio between the region BAPA'B'N (yellow + pink) and ECPC'E'N (yellow + blue) at different  $a/\delta$  values. (B) Graphical illustration of the interpenetration + compression domain.

Table 1. Expressions for Volumes of Different Domains

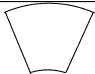

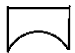


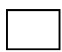


	$V_{1,S} = \frac{2\pi}{3} \left[ 1 - \frac{a^3}{(a+\delta)^3} \right] (a+\delta)^2 (\delta-H)$	(22)
	$V_{2,FP} = \pi\delta(\delta-H)[2a+H-\delta]$	(23)
	$V_3 = \frac{\pi}{3} (\delta-H)[-2\delta^2 + \delta H + H^2 + 3a(\delta+H)]$	(24)
	$V_4 = \frac{\pi}{3} [(-2\delta+H)^2(\delta+H) + 3a(2\delta^2 - 2\delta H + H^2)]$	(25)

Table 2. Dimensionless Expression for Volumes of Different Domains

	$V_{1,S} = \delta^3 \tilde{V}_{1,S} = \delta^3 \left[ \frac{2\pi}{3} \frac{3\tilde{a}^2 + \tilde{a}^2 + 1}{\tilde{a} + 1} (1 - \tilde{H}) \right]$	(22')
	$V_{2,FP} = \delta^3 \tilde{V}_{2,FP} = \delta^3 \pi [(1 - \tilde{H})(2\tilde{a} + \tilde{H} - 1)]$	(23')
	$V_3 = \delta^3 \tilde{V}_3 = \delta^3 \left[ \frac{\pi}{3} (1 - \tilde{H})(\tilde{H}^2 + 3\tilde{H}\tilde{a} + \tilde{H} + 3\tilde{a} - 2) \right]$	(24')
	$V_4 = \delta^3 \tilde{V}_4 = \delta^3 \left[ \frac{\pi}{3} (\tilde{H} - 2)^2 (\tilde{H} + 1) + 3\tilde{a}(2 - 2\tilde{H} + \tilde{H}^2) \right]$	(25')

blue) in Figure 5A. Substituting the volume of region BAPA'B'N (pink + yellow) by that of the region ECPC'E'N (yellow + blue) in the compression domain appears to be satisfactory as long as  $a/\delta > 2$  (Figure 5B). When  $a/\delta$  is small, the approximation underestimates the volume being affected by geometric constraint. However, such underestimation may be partially compensated by the fact that, the deformation is very small near the fringe of the impacted region (AB and A'B') where the geometric restraint is weaker, and that the polymer can squeeze laterally to the red region.

With such simplifying assumptions, we further define the volume of domain BAQA'B'N (green + yellow + pink) as  $V_{1,S}$ , the volume of domain EME'CP'C (yellow + blue + white) as  $V_{2,FP}$ , the volume of domain ECPC'E'N (yellow + blue) as  $V_3$ , and finally the volume of domain GACDE (G'A'C'D'E', red + pink) as  $V_4$ , keeping in mind that all these volumes are a function of separation distance  $H$ . The calculation of these volumes is tedious but straightforward, and the results are listed in Table 1.

Assuming that the polymers are always uniformly distributed in the compressed domain, with the expressions for the volumes in Table 1, the segment density of the polymer in the compressed domain is given as

$$\phi_{S,avg,H} = \phi_{S,avg,\infty} \frac{V_{1,S}}{V_3} \quad (26)$$

for the compressed region of coating on the particle and as

$$\phi_{FP,H} = \phi_{FP,\infty} \frac{V_{2,FP}}{V_3} \quad (27)$$

for the compressed region of coating on the flat plate. It should be noticed that the segment density for both the particle and the plate in region  $V_4$  remains as that in the unperturbed state (i.e.,  $\rho_{S,avg,H}$  and  $\rho_{FP,\infty}$ ). Now eq 19 can be rewritten as

$$\Delta G_{mix,SP}(H) = k_B T \left( \frac{V_p^2}{v_s} \right) \left( \frac{1}{2} - \chi \right) \left( \frac{(\phi_{S,avg,\infty} V_{1,S} + \phi_{FP,\infty} V_{2,FP})^2}{V_3} - \phi_{S,avg,\infty}^2 V_{1,S} - \phi_{FP,\infty}^2 V_{2,FP} + 2\phi_{S,avg,\infty} \phi_{FP,\infty} V_4 \right) \quad (28)$$

Since  $\rho_{FP,\infty}$  and  $\rho_{S,avg,\infty}$  are known through eqs 7 and 17, respectively, eq 28 can be written as

$$\Delta G_{mix,SP}(H) = k_B T \left( \frac{V_p^2}{v_s} \right) \left( \frac{1}{2} - \chi \right) \left( \frac{\gamma n}{\delta} \right)^2 \times \left( \frac{(\eta V_{1,S} + V_{2,FP})^2}{V_3} - \eta^2 V_{1,S} - V_{2,FP} + 2\eta V_4 \right) \quad (29)$$

Equations 28 and 29, which incorporate both the effects of interpenetration and intrapenetration (self-mixing), are only applicable for  $0 \leq H < \delta$  as the volumes given by eqs 22–25 are physically meaningful only in this range. Although we have a simple expression for steric interaction in the interpenetration (only) domain that captures the characteristic of radial nonuniformity (eq 13), we adopt the expressions based on the uniform segment density assumption for both the interpenetration (only) and compression domain for consistency and the continuity of interaction energy at  $H = \delta$ .

It is further noticed that equations in table 1 can be rewritten as products of  $\delta^3$  and functions of normalized variables  $\tilde{a} = a/\delta$  and  $\tilde{H} = H/\delta$  (the compression level):

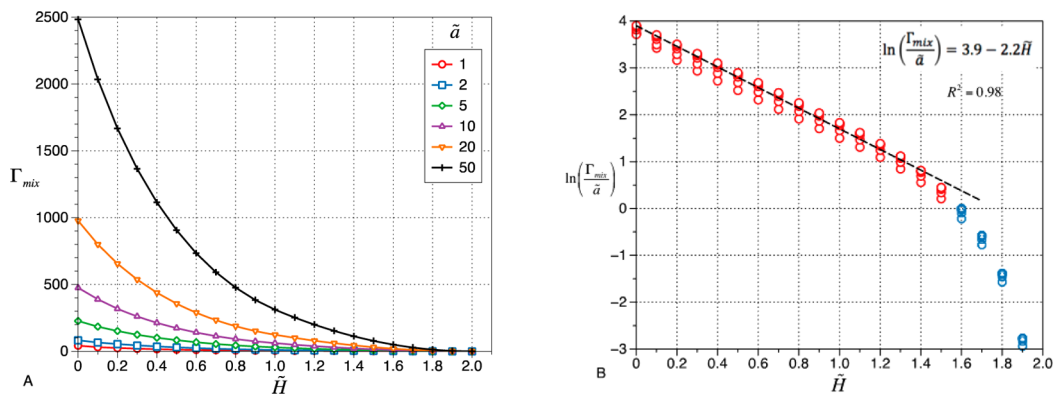


Figure 6. (A)  $\Gamma_{\text{mix}}(\tilde{H})$  as a function of  $\tilde{H}$  at different  $\tilde{a}$ . (B)  $\ln(\Gamma_{\text{mix}}(\tilde{H})/\tilde{a})$  as a function of  $\tilde{H}$ .

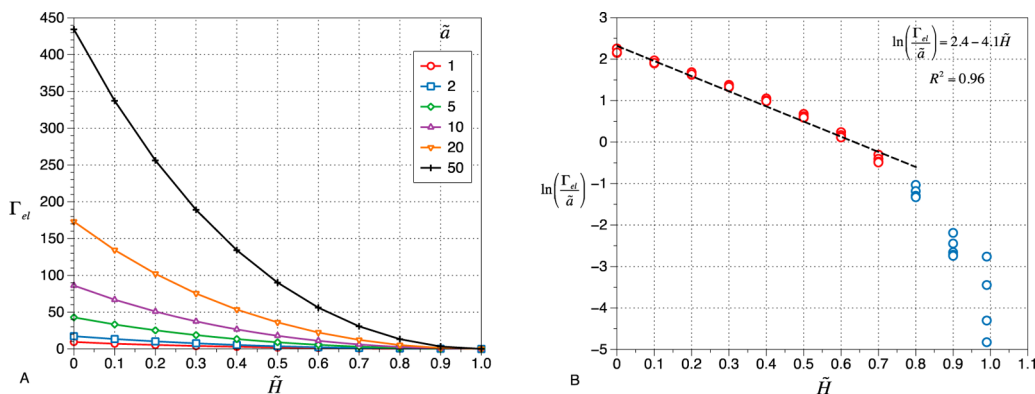


Figure 7. (A)  $\Gamma_{\text{el}}(\tilde{H})$  as a function of  $\tilde{H}$  at different  $\tilde{a}$ . (B)  $\ln(\Gamma_{\text{el}}(\tilde{H})/\tilde{a})$  as a function of  $\tilde{H}$ .

The curvature correcting parameter  $\eta$  can also be expressed as a function of the dimensionless radius  $\tilde{a}$

$$\eta = \frac{3\tilde{a}^2}{3\tilde{a}^2 + 3\tilde{a} + 1} \quad (30)$$

Combining eq 19 and 29 with the dimensionless volumes  $\tilde{V}$  in Table 2, we propose the following expression for the osmotic component of steric interaction:

$$\Delta G_{\text{mix,SP}} = k_{\text{B}}T \left( \frac{V_{\text{p}}^2}{v_{\text{s}}} \right) \left( \frac{1}{2} - \chi \right) (\gamma n)^2 \delta \frac{2}{3} \pi (2 - \tilde{H})^2 (\tilde{H} + 3\tilde{a} + 1) \eta \quad 1 < \tilde{H} \leq 2 \quad (19')$$

$$\Delta G_{\text{mix,SP}} = k_{\text{B}}T \left( \frac{V_{\text{p}}^2}{v_{\text{s}}} \right) \left( \frac{1}{2} - \chi \right) (\gamma n)^2 \delta \left[ \frac{(\eta \tilde{V}_{1,\text{S}} + \tilde{V}_{2,\text{FP}})^2}{\tilde{V}_3} - \eta^2 \tilde{V}_{1,\text{S}} - \tilde{V}_{2,\text{FP}} + 2\eta \tilde{V}_4 \right] \quad 0 < \tilde{H} \leq 1 \quad (29')$$

We notice that these two expressions can both be simply written as the product of a term ( $\lambda$ ) that is characteristic of the polymer coating

$$\lambda_{\text{mix}} = k_{\text{B}}T \left( \frac{V_{\text{p}}^2}{v_{\text{s}}} \right) \left( \frac{1}{2} - \chi \right) (\gamma n)^2 \delta \quad (31)$$

and a term ( $\Gamma$ ) that is characteristic of the geometry of interaction

$$\Gamma_{\text{mix}}(\tilde{H}) = \begin{cases} \frac{2}{3} \pi (2 - \tilde{H})^2 (\tilde{H} + 3\tilde{a} + 1) \eta & 1 < \tilde{H} \leq 2 \\ \frac{(\eta \tilde{V}_{1,\text{S}} + \tilde{V}_{2,\text{FP}})^2}{\tilde{V}_3} - \eta^2 \tilde{V}_{1,\text{S}} - \tilde{V}_{2,\text{FP}} + 2\eta \tilde{V}_4 & 0 < \tilde{H} \leq 1 \end{cases} \quad (32)$$

Therefore, the osmotic contribution to the steric interaction energy is simply

$$\Delta G_{\text{mix,SP}}(\tilde{H}) = \lambda_{\text{mix}} \Gamma_{\text{mix}}(\tilde{H}) \quad (33)$$

Plotting  $\Gamma_{\text{mix}}(\tilde{H})$  vs  $\tilde{H}$  (Figure 5A) reveals that  $\Gamma_{\text{mix}}(\tilde{H})$  may be approximated by a simple exponential decay function the magnitude of which is controlled by  $\tilde{a}$ . We therefore propose the simple approximation for  $\Gamma_{\text{mix}}(\tilde{H})$  as the following:

$$\Gamma_{\text{mix}}(\tilde{H}) = k_1 \tilde{a} \exp(-k_2 \tilde{H}) \quad (34)$$

To find the constants  $k_1$  and  $k_2$ , we can plot  $\ln(\Gamma_{\text{mix}}(\tilde{H})/\tilde{a})$  against  $\tilde{H}$ , in which case eq 32 becomes

$$\ln \left( \frac{\Gamma_{\text{mix}}(\tilde{H})}{\tilde{a}} \right) = k_1 - k_2 \tilde{H} \quad (35)$$

The expression obtained via a linear regression is

$$\Gamma_{\text{mix}}(\tilde{H}) = 49.4 \tilde{a} \exp(-2.2 \tilde{H}) \quad (36)$$

Note that the linear regression was conducted only for  $\tilde{H} \leq 1.5$  as this is the range that allows for a good fit ( $R = 0.99$ ) and outside this range  $\Gamma_{\text{mix}}(\tilde{H})$  is negligibly small anyway (see Figure 7A and also note the fact that the y axis in Figure 7B is log-scaled). Thus, a simple exponential decay function is



**Table 3. Effective Thickness ( $\delta$ ),  $\lambda_{\text{osm}}$  and  $l$  for Polymer Coatings of Different Configurations (Brush and Blob) in a Good Solvent<sup>a</sup>**

	brush		blob (mushroom)	
$\delta$	$\delta \approx nl^{5/3}\gamma^{1/3}$	(44) <sup>35</sup>	$\delta \approx R_F \approx n^{3/5}l$	(45) <sup>34</sup>
$\lambda_{\text{mix}}(k_B T)$	$\left(\frac{V_p^2}{v_s}\right)\left(\frac{1}{2} - \chi\right)n^3\gamma^{7/3}l^{5/3}$	(46)	$\left(\frac{V_p^2}{v_s}\right)\left(\frac{1}{2} - \chi\right)n^{13/5}\gamma^2 l$	(47)
$\lambda_{\text{el}}(k_B T)$	$n^2\gamma^{5/3}l^{10/3}$	(48)	$n^{6/5}\gamma l^2$	(49)

<sup>a</sup> $l$  = segmental length of polymer.  $s$  = mean distance between polymer chains on the surface ( $s = (1/\gamma)^{1/2}$ ).  $R_F$  = Flory radius of a polymer blob in a good solvent.

predicted to approximate an interaction that involves a rather complicated change in geometry.

Lastly, it is important to point out that, although eq 36 seems universal to all sphere-plate geometry (the only requirement is that the coating layers are of the same thickness), it is universal only if  $\Gamma_{\text{mix}}(\tilde{H})$  is written as a function of dimensionless separation distance. However, in experimental practice, the actual data are usually plotted as energy or force versus  $H$  (absolute separation distance), in which case the exponential decay constant is a function of the coating thickness.

### ■ ELASTIC CONTRIBUTION

According to the theory of Flory,<sup>33,34</sup> the elastic contribution to the Gibbs free energy of steric interaction from the compression of the spherical shell can be approximated by

$$\begin{aligned}\Delta G_{\text{el}}^s &= -k_B T A_S \gamma \ln\left(\frac{V_{S,f}}{V_{S,i}}\right) \approx -k_B T A_S \gamma \ln\left(\frac{V_3}{V_{1,S}}\right) \\ &= k_B T \gamma \delta^2 \left(2\pi \tilde{a}^2 \frac{1 - \tilde{H}}{1 + \tilde{a}}\right) \\ &\quad \ln\left(\frac{2\tilde{a}^2 + 3\tilde{a} + 1}{\tilde{H}^2 + 3\tilde{H}\tilde{a} + \tilde{H} + 3\tilde{a} - 2}\right) \quad 0 < \tilde{H} \leq 1\end{aligned}\quad (37)$$

where  $V_{S,f}$  and  $V_{S,i}$  are the final and initial volumes involved in the compression for the spherical shell coating. Accordingly, the elastic contribution to the Gibbs free energy of steric interaction from the compression of the coating on the flat plate can be approximated by

$$\begin{aligned}\Delta G_{\text{el}}^{\text{FP}} &= -k_B T A_{\text{FP}} \gamma \ln\left(\frac{V_{\text{FP},f}}{V_{\text{FP},i}}\right) \approx -k_B T A_{\text{FP}} \gamma \ln\left(\frac{V_3}{V_{2,\text{FP}}}\right) \\ &= k_B T \gamma \delta^2 \pi (1 - \tilde{H})(2\tilde{a} + \tilde{H} - 1) \\ &\quad \ln\left(\frac{3(2\tilde{a} + \tilde{H} - 1)}{(\tilde{H}^2 + 3\tilde{H}\tilde{a} + \tilde{H} + 3\tilde{a} - 2)}\right) \quad 0 < \tilde{H} \leq 1\end{aligned}\quad (38)$$

where  $V_{\text{FP},f}$  and  $V_{\text{FP},i}$  are the final and initial volumes involved in the compression for the coating on the flat surface. The total Gibbs free energy for the elastic contribution to steric interaction would then be given by

$$\Delta G_{\text{el}}^{\text{total}} = \Delta G_{\text{el}}^s + \Delta G_{\text{el}}^{\text{FP}} \quad 0 < \tilde{H} \leq 1 \quad (39)$$

Again we can rewrite eq 39 as a product of a term that is characteristic of the coating layer

$$\lambda_{\text{el}} = k_B T \gamma \delta^2 \quad (40)$$

and a term that is characteristic of the geometry

$$\Gamma_{\text{el}}(\tilde{H}) = \begin{cases} 2\pi \tilde{a}^2 \frac{1 - \tilde{H}}{1 + \tilde{a}} \ln\left(\frac{2\tilde{a}^2 + 3\tilde{a} + 1}{(\tilde{H}^2 + 3\tilde{H}\tilde{a} + \tilde{H} + 3\tilde{a} - 2)}\right), & \text{sphere} \\ \pi(1 - \tilde{H})(2\tilde{a} + \tilde{H} - 1) \ln\left(\frac{3(2\tilde{a} + \tilde{H} - 1)}{(\tilde{H}^2 + 3\tilde{H}\tilde{a} + \tilde{H} + 3\tilde{a} - 2)}\right), & \text{plate} \end{cases}$$

when  $0 < \tilde{H} \leq 1$  (41)

Similarly, we can plot  $\Gamma_{\text{el}}$  and  $\ln(\Gamma_{\text{el}}(\tilde{H})/\tilde{a})$  as a function of  $\tilde{H}$  and the results are shown in Figure 7. It is observed that for range where the elastic interaction is significant ( $\tilde{H} \leq 0.8$ ), the geometric term  $\Gamma_{\text{el}}$  can be sufficiently described as

$$\Gamma_{\text{el}}(\tilde{H}) = 11.0\tilde{a} \exp(-4.1\tilde{H}) \quad (42)$$

Again the elastic contribution to the steric interaction between a sphere and a flat plate can be approximated by a simple exponentially decaying function. Comparing eqs 36 and 42, we found that the elastic contribution decays faster with increasing separation distance than the osmotic contribution.

### ■ RELATIVE CONTRIBUTIONS FROM OSMOTIC AND ELASTIC INTERACTION

Up to this point we have only discussed the geometrically related changes during the interaction. We have derived approximate expressions for  $\Gamma_{\text{mix}}$  and  $\Gamma_{\text{el}}$  that capture the characteristics of osmotic and elastic interactions when the coated particle approaches the coated surface. However, it is important to understand the overall strength of the interaction, the relative strengths of the different contributions to the interaction, and the factors affecting them. The major difference between the  $\Gamma_{\text{mix}}$  and  $\Gamma_{\text{el}}$ , other than their magnitudes, is that  $\Gamma_{\text{mix}}$  depends on the property of the solvent, whereas  $\Gamma_{\text{el}}$  does not. Since the expressions for  $\Gamma_{\text{mix}}$  (eq 31) and  $\Gamma_{\text{el}}$  (eq 40) still contain a geometric parameter  $\delta$  (coating thickness), we can relate  $\delta$  to the degree of polymerization  $n$  by defining

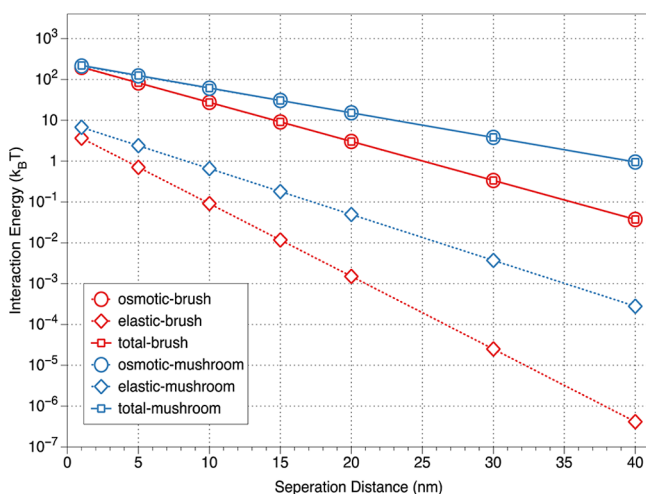
$$\delta = f(n) \quad (43)$$

Depending on the fixation mode (i.e., whether the polymers exist on the surface as mushroom, brush or other configurations),  $f(n)$  can assume different mathematical forms. The effective coating thicknesses ( $\delta$ ) and the corresponding prefactors for osmotic contribution ( $\lambda_{\text{mix}}$ ) and elastic contribution ( $\lambda_{\text{el}}$ ) for two different configurations (brush and mushroom models) are listed in Table 3.

It should be noted that for polymer adsorbing onto the surface as blobs, the number of polymer chains per area ( $\gamma$ ) theoretically can not exceed  $1/R_F^2$ . For polymer brush, such limitation do not exist, but the thickness is related to  $\gamma$  by eq 44.

It is also proposed that the “mushroom” model is more appropriate when the surface coverage is low ( $R_F < s$ ) and the “brush” model is more appropriate when the surface coverage is high ( $R_F > s$ ).<sup>36</sup> However, evaluating the total interaction energy (osmotic + elastic) over a large range of  $\gamma$  reveals that the difference between the maximum interaction energy from both models is always less than 15%, although the “mushroom” model predicts a slower decay of interaction with increasing separation distance.

Figure 8 shows a set of sample energy curves for the total steric interaction energy and its osmotic and elastic



**Figure 8.** Potential energy for steric interaction between a sphere of  $a = 50$  nm and a plate. The parameters for calculation are as follows:  $\chi = 0.2$ ,  $n = 100$ ,  $\gamma = 0.001 \text{ nm}^{-2}$ ,  $l = 1 \text{ nm}$ ,  $V_p = 1 \text{ nm}^3$ ,  $\nu_s = 0.03 \text{ nm}^3$ . With these parameters,  $R_F \approx 15.8 \text{ nm} < s \approx 31.6 \text{ nm}$ , and thus the mushroom model may be more appropriate.

contributions respectively. Both the models based on “brush” and “mushroom” configurations are used to evaluate the interaction energy. In both cases the elastic contribution is always at least an order of magnitude lower than the osmotic contribution to the total steric interaction energy throughout the interaction.

### ■ COATING POLYMER ON THE PARTICLE ONLY

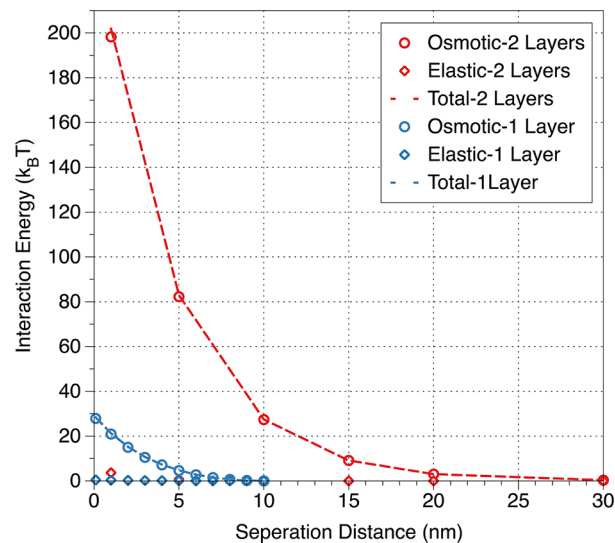
The recent concern in environmental and health safety of nanomaterials<sup>37</sup> has spurred research interest in better understanding the colloidal interaction between nanoparticles, many of which are coated with polymer, and environmental surfaces that might not be subject to similar surface modification.<sup>38,39</sup> A similar scenario where uncoated particles interacting with a polymer modified flat surface has also been studied.<sup>40,41</sup> In such scenarios, the steric interaction can be significantly undermined due to the absence of interpenetration of polymer layers. However, due to the compression of the polymer layer when  $H < \delta$ , osmotic contribution due to intrapenetration (self-mixing) and elastic contribution still remain significant. The interaction energy due to intrapenetration ( $\Delta G_{\text{self-mix}}^S$ ) can be evaluated using eq 50, which is simply derived from the Flory–Krigbaum theory with  $\phi_{\text{FP},\infty} = 0$ .

$$\Delta G_{\text{self-mix}}^S = k_B T \left( \frac{V_p^2}{\nu_s} \right) \left( \frac{1}{2} - \chi \right) \phi_{s,\text{avg},\infty}^2 V_{1,s} \left( \frac{V_{1,s}}{V_3} - 1 \right) \quad (50)$$

$H \leq \delta$

The elastic contribution ( $\Delta G_{\text{el}}^S$ ) to the interaction energy can be described by expression 38. The total steric interaction is then the sum of  $\Delta G_{\text{self-mix}}^S$  and  $\Delta G_{\text{el}}^S$ .

With the exact same parameters for the spherical particle and its coating layer as those to produce Figure 8, the total steric interaction energy and its osmotic and elastic contributions are plotted in Figure 9. Comparing the results between Figures 8



**Figure 9.** Comparison between the potential energy for (red) an interaction between a sphere of  $a = 50$  nm coated with polymers and a flat plate coated with same polymers; (blue) an interaction between a sphere of  $a = 50$  nm coated with polymers and a bare flat plate. The parameters for the polymer coatings are the same as those in Figure 8.

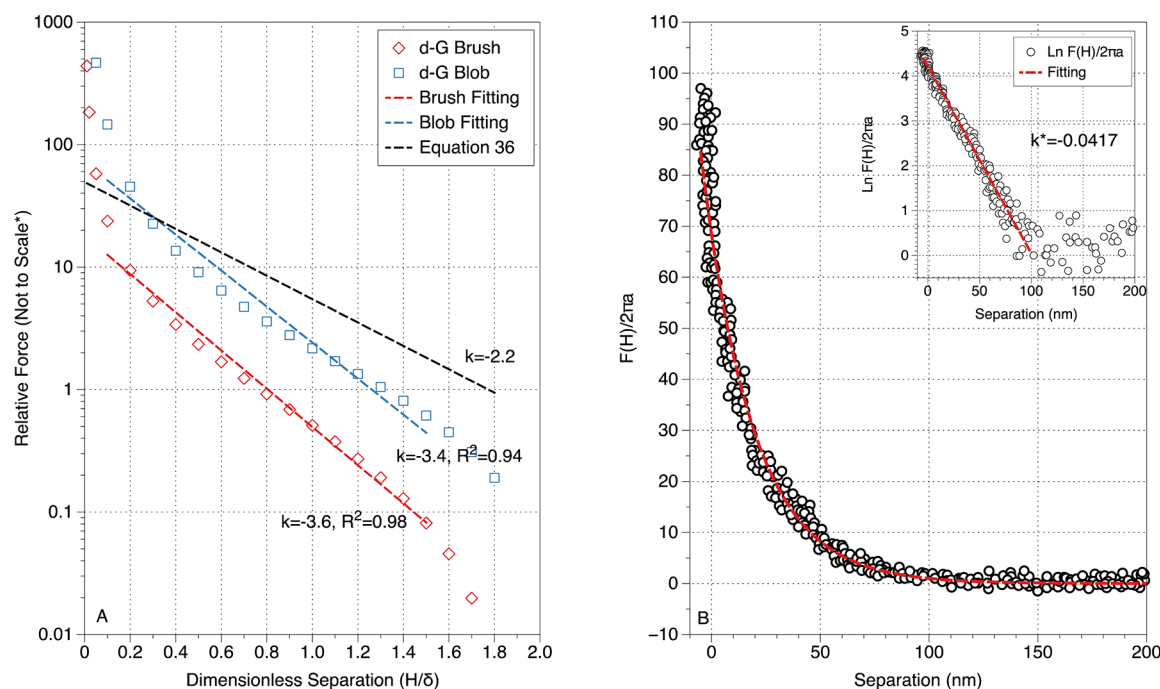
and 9 shows that the absence of polymer coating on the flat plate decreases the steric interaction energy by nearly an order of magnitude, emphasizing the importance of the presence of polymeric coatings on both the interacting surfaces in imparting effective steric interaction.<sup>38</sup> Finally, it should again be noted that, even without interpenetration, the elastic contribution still only composes a very small fraction of the total interaction energy, as compared to the self-penetration mechanism as the major contributor.

### ■ COMPARISON WITH EXISTING MODELS AND MODEL VALIDATION

There was no present model specifically developed for a sphere–plate interaction as the existing models were mainly established for the plate–plate interaction, or in limited cases, for the sphere–sphere interaction. Therefore, the “existing models” mentioned here are referred to sphere–plate models scaled from the plate–plate models by simply employing DA as given by eq 2.

Two commonly used expressions for describing the steric force per area between two pair parallel flat plates were given by de Gennes as the following:<sup>17</sup>

brush model



**Figure 10.** (A) Different modes of decay of interaction energy with increasing separation. The black line represents the approximate expression derived (eq 36). The exact evaluations of eqs 53 and 54 are presented as blue square and red diamonds, respectively, with the blue and red dotted lines being the exponential fittings for the midrange interaction ( $\tilde{H} = 0.1$  to  $1.5$ ). (B) Normalized force profile determined experimentally (black circles) and the exponential fit with the proposed model (red dotted line). The same data and fitting are presented in the inset with the y axis in a natural-log scale. The fitting is based on eq 55 with a slight adjustment in x axis (9 nm left shift), which is reasonable because the absolute separation between the probe and the plate is undetermined as reported in the original publication.<sup>48</sup>

$$\frac{F_{\text{pp,brush}}(h)}{k_{\text{B}}T} = \frac{1}{s^3} \left[ \left( \frac{2\delta}{h} \right)^{9/4} - \left( \frac{h}{2\delta} \right)^{3/4} \right] \quad h < 2\delta \quad (51)$$

blob (mushroom) model

$$\frac{F_{\text{pp,blob}}(h)}{k_{\text{B}}T} = \frac{1}{2s^2\delta} \left( \frac{\delta}{h} \right)^{8/3} \quad h < 2\delta \quad (52)$$

where  $s$  is the average distance between attachment points ( $s \propto \sqrt{\gamma}$ ),  $\delta$  is the coating thickness, and  $h$  is the separation distance between two flat plates. To obtain the potential energy of a sphere-plate interaction, we can simply integrate the above force expression from infinity to a given separation  $H$  to yield the per area potential energy of steric interaction between two flat plates, then apply the DA (eq 2). For comparison with the experimental results, it may be more convenient use the force profiles rather than the energy profiles, as force profiles are usually what the experimental results are recorded as. The detailed derivations of the expressions for both force and energy profiles are given in the Supporting Information, whereas the resulting force expressions are presented below:

brush

$$\frac{F_{\text{SP,brush}}(\tilde{H})}{k_{\text{B}}T} \approx 17.28 \frac{a\delta}{s^3} [1 - 1.39\tilde{H}^{-5/4} - 0.12\tilde{H}^{7/4}] \quad \tilde{H} < 2 \quad (53)$$

blob

$$\frac{F_{\text{SP,blob}}(\tilde{H})}{k_{\text{B}}T} \approx 3.77 \frac{a}{s^2} [-1 + 3.17\tilde{H}^{-5/3}] \quad \tilde{H} < 2 \quad (54)$$

The expressions in the brackets of eqs 53 and 54, which are only dependent on compression level  $\tilde{H}$ , are plotted as red diamond and blue circles in Figure 10A, respectively. The structures of eqs 51–54 reveal that the steric force becomes infinity at zero separation. This is theoretically reasonable for a plate–plate interaction (eqs 51 and 52) as the segment density becomes infinity upon zero separation. However, with a sphere–plate interaction, the possibility of chain tilting and/or lateral movement lead to finite segment density even at zero separation. Consequentially, the steric interaction force (energy) is finite for a sphere–plate interaction, which is not predicted by models applying DA but by our proposed model (eq 32) and its approximate form (eq 36). With both the brush and the blob (mushroom) models, the decays are not exponential for the entire interaction range. However, reasonably good exponential fittings can be applied to both interactions from  $\tilde{H} = 0.1$  to  $1.5$ , leading to thickness-normalized decay rates of  $-3.4$  for the blob model and  $-3.6$  for the brush model. Also plotted in Figure 10A is the exponential term of the derived model as described by eq 36 with a decay rate of  $-2.2$ . Because it has been shown in Figure 8 that the elastic contribution is always more than 1 order of magnitude lower than the osmotic contribution, for simplicity, only the osmotic contribution, which is described by eq 36, is considered for comparison with the other models. It should be noted that Figure 10A only intends to show the comparison of decay rates between different models whereas the relative magnitudes of the interaction energy are not to scale in the figure, because the magnitudes are also determined by the prefactors in the corresponding equations.

Most experiments for the measurement of steric interaction energy were conducted using surface force apparatus

(SFA)<sup>42–47</sup> the “cross-cylinder” geometry of which is not exactly the same as the “sphere-plate” geometry involved in this study. A study by Braithwaite et al.,<sup>48</sup> which utilized a high-resolution modified atomic force microscope (m-AFM) to study the effect of poly ethylene oxide (PEO) adsorption on the interaction between a spherical probe and a flat substrate, provides an interaction of sphere-plate geometry for the validation of the proposed model. In the reported study the interaction was monitored in an aqueous solution of 250 mM KNO<sub>3</sub> that yields a Debye length of about 0.6 nm. Therefore, the electrical double layer interaction is negligible over the range of interaction.

The data is extracted from the original publication (“separation in” in Figure 8 on Braithwaite’s article)<sup>48</sup> using an image digitizing software (Plot Digitizer) and is shown in Figure 10B. Using a y axis of natural-logarithm scale reveals that the decay is exponential throughout the entire range of interaction, with a decay rate of  $-0.042$  and an interaction range (i.e.,  $2\delta$ ) of around 100 nm. Because the decay rates in Figure 10A are normalized by the coating thickness ( $\delta$ ), it is justified to calculate  $\delta$  as the ratio between the normalized decay rate ( $k$ ) and the absolute decay rate ( $k^*$ ). With this approach, the  $\delta$  is calculated to be 52.8, 81.5, and 86.3 nm with three different models as described by eqs 36, 53, and 54 correspondingly. It is clear that the model described by eq 36 predicts a coating thickness more consistent with the measured value as shown in Figure 10B inset ( $\sim 50$  nm). Using a Kuhn segment length of  $l = 0.8$ ,<sup>49,50</sup> the effective coating thickness is estimated to be 58.3 nm based on the blob model as described by eq 45.

By taking the derivative of the interaction energy (eq 33, which is a combination of eqs 31 and 36) with respect to separation distance, the following expression describing the force profile can be obtained:

$$\frac{F(\tilde{H})}{k_B T} \approx 108.7 \left( \frac{V_p^2}{v_s} \right) \left( \frac{1}{2} - \chi \right) (\gamma n)^2 \frac{a}{\delta} \exp \left( -2.2 \frac{H}{\delta} \right) \quad H \geq 2\delta \quad (55)$$

With the following parameters ( $\chi = 0.46$ ,  $n = 1272$ ,  $V_p = 0.69$  nm<sup>3</sup>,  $v_s = 0.03$  nm<sup>3</sup>,  $\delta = 52$  nm),<sup>51,52</sup> we estimate the area density of the polymer chains to be  $\gamma \approx 2.7 \times 10^{-4}$  nm<sup>-2</sup>. As mentioned earlier, for the blobs formed by polymer adsorption onto surfaces,  $\gamma$  cannot exceed  $1/R_F^2 \approx 1/(n^{3/5}l)^2 \approx 2.9 \times 10^{-4}$  nm<sup>-2</sup>. The value estimated from the interaction curve is very close to this limit, which is consistent with the fact that equilibrium had reached for the adsorption of PEO to the interacting surfaces.<sup>48</sup>

## CONCLUDING REMARKS

We have shown that the curvature of the core of a colloidal particle can drastically change the distribution of segment density of its polymer-coating layer and consequentially undermines the steric interaction between a spherical particle and a flat surface. We have also shown the inherent problem of applying DA in calculating steric interaction for a sphere–plate interaction. Not only does DA overestimate the steric interaction energy/force, in the extreme scenario of zero separation it predicts infinite interaction energy/force that is unrealistic.

Expressions are derived for the osmotic (mixing) and elastic contributions of steric interaction between a particle and a flat surface (sphere-plate interaction).

The energy of mixing is given by applying the Flory–Krigbaum theory to the geometry change associated with interpenetration and compression during the interaction assuming a constant segment density throughout the polymer layer. It was found that (1) both the osmotic and elastic contribution can be satisfactorily approximated by exponential functions and (2) the elastic contribution is always more than 1 order of magnitude lower than the osmotic contribution, regardless whether a brush model or blob model is applied, or whether the polymer coating is present on only one or both of the interacting surfaces. With the proposed approximate expressions (i.e., eqs 31, 33, and 36 for energy of osmotic contribution; or equivalently eq 55 for the force), we are able to fit reported experimental data obtained from distance-dependent steric force measurements conducted using a high resolution AFM. The proposed expressions in their simple exponential form may facilitate the estimation of potential energy of steric interaction between colloidal particles (nanoparticles) and a substrate surface, which is important in determining the affinity between the colloidal particles and the surface.

## ASSOCIATED CONTENT

### Supporting Information

Derivations of eqs 53 and 54 based on the de Gennes model on steric interaction between two flat plates. This material is available free of charge via the Internet at <http://pubs.acs.org>.

## AUTHOR INFORMATION

### Corresponding Author

\*E-mail: [wiesner@duke.edu](mailto:wiesner@duke.edu). Phone: 919-660-5292. Fax: 919-660-5219.

### Notes

The authors declare no competing financial interest.

## ACKNOWLEDGMENTS

This material is based upon work supported by the National Science Foundation (NSF) and the Environmental Protection Agency (EPA) under NSF Cooperative Agreement EF-0830093, Center for the Environmental Implications of NanoTechnology (CEINT). Any opinions, findings, conclusions, or recommendations expressed in this material are those of the author(s) and do not necessarily reflect the views of the NSF or the EPA. This work has not been subjected to EPA review and no official endorsement should be inferred.

## REFERENCES

- (1) Hunter, R. J. *Foundations of colloid science*; Oxford University Press: New York, 2001.
- (2) Hiemenz, P. C.; Rajagopalan, R. *Principles of colloid and surface chemistry*; CRC: Boca Raton, FL, 1997.
- (3) Napper, D. H. Steric stabilization. *J. Colloid Interface Sci.* **1977**, *58*, 390–407.
- (4) Fritz, G.; Schädler, V.; Willenbacher, N.; Wagner, N. J. Electrosteric Stabilization of Colloidal Dispersions. *Langmuir* **2002**, *18*, 6381–6390.
- (5) Eiden-Assmann, S.; Widoniak, J.; Maret, G. Synthesis and Characterization of Porous and Nonporous Monodisperse Colloidal TiO<sub>2</sub> Particles. *Chem. Mater.* **2004**, *16*, 6–11.



- (6) Amalvy, J. I.; Unali, G. F.; Li, Y.; Granger-Bevan, S.; Armes, S. P.; Binks, B. P.; Rodrigues, J. A.; Whitby, C. P. Synthesis of sterically stabilized polystyrene latex particles using cationic block copolymers and macromonomers and their application as stimulus-responsive particulate emulsifiers for oil-in-water emulsions. *Langmuir* **2004**, *20*, 4345–4354.
- (7) Tiller, C. Natural organic matter and colloidal stability: Models and measurements. *Colloids Surf., A* **1993**, *89*–102.
- (8) Franchi, A.; O'Melia, C. R. Effects of Natural Organic Matter and Solution Chemistry on the Deposition and Reentrainment of Colloids in Porous Media. *Environ. Sci. Technol.* **2003**, *37*, 1122–1129.
- (9) Hyung, H.; Fortner, J. D.; Hughes, J. B.; Kim, J.-H. Natural Organic Matter Stabilizes Carbon Nanotubes in the Aqueous Phase. *Environ. Sci. Technol.* **2007**, *41*, 179–184.
- (10) Phenrat, T.; Song, J. E.; Cisneros, C. M.; Schoenfelder, D. P.; Tilton, R. D.; Lowry, G. V. Estimating Attachment of Nano- and Submicrometer-particles Coated with Organic Macromolecules in Porous Media: Development of an Empirical Model. *Environ. Sci. Technol.* **2010**, *44*, 4531–4538.
- (11) Chen, K. L.; Elimelech, M. Interaction of Fullerene (C 60) Nanoparticles with Humic Acid and Alginate Coated Silica Surfaces: Measurements, Mechanisms, and Environmental Implications. *Environ. Sci. Technol.* **2008**, *42*, 7607–7614.
- (12) Quevedo, I. R.; Tufenkji, N. Mobility of Functionalized Quantum Dots and a Model Polystyrene Nanoparticle in Saturated Quartz Sand and Loamy Sand. *Environ. Sci. Technol.* **2012**, *46*, 4449–4457.
- (13) Byrd, T. L.; Walz, J. Y. Interaction Force Profiles between *Cryptosporidium parvum* Oocysts and Silica Surfaces. *Environ. Sci. Technol.* **2005**, *39*, 9574–9582.
- (14) Rijnaarts, H. H. M.; Norde, W.; Lyklema, J.; Zehnder, A. J. B. DLVO and steric contributions to bacterial deposition in media of different ionic strengths. *Colloids Surf., B* **1999**, *14*, 179–195.
- (15) Flory, P. J.; Krigbaum, W. R. Statistical Mechanics of Dilute Polymer Solutions. II. *J. Chem. Phys.* **1950**, *18*, 1086–1094.
- (16) Vincent, B.; Edwards, J.; Emmett, S.; Jones, A. Depletion flocculation in dispersions of sterically-stabilised particles ("soft spheres"). *Colloids Surf.* **1986**, *18*, 261–281.
- (17) de Gennes, P. G. Polymers at an interface; a simplified view. *Adv. Colloid Interface Sci.* **1987**, *27*, 189–209.
- (18) Biggs, S. Steric and Bridging Forces between Surfaces Bearing Adsorbed Polymer: An Atomic Force Microscopy Study. *Langmuir* **1995**, *11*, 156–162.
- (19) Huang, H.; Ruckenstein, E. Steric and Bridging Interactions between Two Plates Induced by Grafted Polyelectrolytes. *Langmuir* **2006**, *22*, 3174–3179.
- (20) Derjaguin, B. V.; Landau, L. Theory of the stability of strongly charged lyophobic sols and of the adhesion of strongly charged particles in solutions of electrolytes. *Acta Physicochim. URSS* **1941**, *14*, 633–662.
- (21) Gregory, J. Interaction of unequal double layers at constant charge. *J. Colloid Interface Sci.* **1975**, *51*, 44–51.
- (22) Verwey, E. J. W. Theory of the stability of lyophobic colloid. *J. Phys. Chem.* **1947**, *51*, 631–636.
- (23) Ohshima, H. *Biophysical Chemistry of Biointerfaces*; Wiley: New Jersey, 2010.
- (24) Lin, S.; Wiesner, M. R. Exact Analytical Expressions for the Potential of Electrical Double Layer Interactions for a Sphere–Plate System. *Langmuir* **2010**, *26*, 16638–16641.
- (25) Matsen, M. W. Effect of Chain Tilt on the Interaction between Brush-Coated Colloids. *Macromolecules* **2005**, *38*, 4525–4530.
- (26) Tirrell, M. Polymers tethered to curves interfaces: a self-consistent-field analysis. *Macromolecules* **1992**, *25*, 2890–2895.
- (27) Milner, S. T.; Witten, T. A.; Cates, M. E. Theory of the grafted polymer brush. *Macromolecules* **1988**, *21*, 2610–2619.
- (28) Milner, S. T.; Witten, T. A.; Cates, M. E. Effects of polydispersity in the end-grafted polymer brush. *Macromolecules* **1989**, *22*, 853–861.
- (29) Lin, E. K.; Gast, A. P. Self Consistent Field Calculations of Interactions between Chains Tethered to Spherical Interfaces. *Macromolecules* **1996**, *29*, 390–397.
- (30) Kim, J. U.; Matsen, M. W. Interaction between Polymer-Grafted Particles. *Macromolecules* **2008**, *41*, 4435–4443.
- (31) Lozsan, A.; Garcia-Sucre, M.; Urbina-Villalba, G. Steric interaction between spherical colloidal particles. *Phys. Rev. E* **2005**, *72*.
- (32) Wijmans, C. M.; Zhulina, E. B. Polymer brushes at curved surfaces. *Macromolecules* **1993**, *26*, 7214–7224.
- (33) Evans, R.; Smitham, J. B.; Napper, D. H. Theoretical prediction of the elastic contribution to steric stabilization. *Colloid Polym. Sci.* **1977**, *255*, 161–167.
- (34) Flory, P. J. *Principles of polymer chemistry*; Cornell University Press: Ithaca, NY, 1953.
- (35) Alexander, S. Polymer adsorption on small spheres. A scaling approach. *J. Phys. (Paris)* **1977**, *38*, 977–981.
- (36) Israelachvili, J. N. *Intermolecular And Surface Forces*; Academic Press: New York, 2010.
- (37) Wiesner, M. R.; Lowry, G. V.; Alvarez, P.; Dionysiou, D.; Biswas, P. Assessing the Risks of Manufactured Nanomaterials. *Environ. Sci. Technol.* **2006**, *40*, 4336–4345.
- (38) Lin, S.; Cheng, Y.; Liu, J.; Wiesner, M. R. Polymeric Coatings on Silver Nanoparticles Hinder Autoaggregation but Enhance Attachment to Uncoated Surfaces. *Langmuir* **2012**, *28*, 4178–4186.
- (39) Lin, S.; Wiesner, M. R. Theoretical investigation on the interaction between a soft particle and a rigid surface. *Chem. Eng. J.* **2012**, *191*, 297–305.
- (40) Xu, L.-C.; Logan, B. E. Interaction Forces between Colloids and Protein-Coated Surfaces Measured Using an Atomic Force Microscope. *Environ. Sci. Technol.* **2005**, *39*, 3592–3600.
- (41) Kim, J. U.; Matsen, M. W. Repulsion Exerted on a Spherical Particle by a Polymer Brush. *Macromolecules* **2008**, *41*, 246–252.
- (42) Taunton, H.; Toprakcioglu, C.; Fetters, L. Interactions between surfaces bearing end-adsorbed chains in a good solvent. *Macromolecules* **1990**, *23*, 571–580.
- (43) Kuhl, T.; Leckband, D.; Lasic, D. Modulation of interaction forces between bilayers exposing short-chained ethylene oxide headgroups. *Biophys. J.* **1994**, *66*, 1479–1488.
- (44) Luckham, P. F.; Klein, J. Forces between mica surfaces bearing adsorbed polyelectrolyte, poly-L-lysine, in aqueous media. *J. Chem. Soc., Faraday Trans. 1* **1984**, *80*, 865–878.
- (45) Luckham, P. F.; Klein, J. Forces between mica surfaces bearing adsorbed homopolymers in good solvents. The effect of bridging and dangling tails. *Faraday Trans.* **1990**, *86*, 1363–1368.
- (46) Taunton, H. J.; Toprakcioglu, C.; Klein, J. Direct measurement of the interaction between mica surfaces with adsorbed diblock copolymer in a good solvent. *Macromolecules* **1988**, *21*, 3333–3336.
- (47) Luckham, P. Forces between two adsorbed polyethylene oxide layers immersed in a good aqueous solvent. *Nature* **1982**, *300*, 429–431.
- (48) Braithwaite, G. J. C.; Howe, A.; Luckham, P. F. Interactions between Poly(ethylene oxide) Layers Adsorbed to Glass Surfaces Probed by Using a Modified Atomic Force Microscope. *Langmuir* **1996**, *12*, 4224–4237.
- (49) Mattea, C.; Fatkullin, N.; Fischer, E.; Beginn, U. The "corset effect" of spin-lattice relaxation in polymer melts confined in nanoporous media. *Appl. Magn. Reson.* **2004**, *27*, 371–381.
- (50) Kimmich, R.; Fatkullin, N.; Mattea, C.; Fischer, E. Polymer chain dynamics under nanoscopic confinements. *Magn. Reson. Imaging* **2005**, *23*, 191–196.
- (51) Hermans, J. Excluded volume theory of polymer-protein interactions based on polymer chain statistics. *J. Chem. Phys.* **1982**, *77*, 2193.
- (52) Dormidontova, E. E. Role of competitive PEO-water and water-water hydrogen bonding in aqueous solution PEO behavior. *Macromolecules* **2002**, *35*, 987–1001.



**■ NOTE ADDED AFTER ASAP PUBLICATION**

This paper was published on the Web on Oct 16, 2012, with an error in Figure 6. The corrected version was reposted on Oct 17, 2012.